ChemComm

Accepted Manuscript

This article can be cited before page numbers have been issued, to do this please use: J. B. Lee, M. E. Kang, J. Kim, C. Y. Lee, J. Kee, K. Myung, J. U. Park and S. Y. Hong, *Chem. Commun.*, 2017, DOI: 10.1039/C7CC05794F.

ROYAL SOCIETY OF CHEMISTRY

rsc.li/chemcomm

View Article Online
DOI: 10.1039/C7CC05794F

Journal Name

COMMUNICATION

Direct diversification of unmasked quinazolin-4(3*H*)-ones through orthogonal reactivity modulation

Received 00th January 20xx,
Accepted 00th January 20xx

DOI: 10.1039/x0xx00000x

www.rsc.org/

Jae Bin Lee,[a] Mi Eun Kang,[a] Joohee Kim,[b] Chang Young Lee,[a] Jung-Min Kee,[c] Kyungjae Myung,[d] Jang-Ung Park*[b] and Sung You Hong*[ad]

Here we report a set of direct functionalization methods of unmasked 2-phenylquinazolin-4(3*H*)-ones, a privileged alkaloid core, without the installation/removal event of protecting groups or exogenous coordinating moieties. Divergent pathways were modulated with transition-metal catalysts by suppressing competitive reactivities, leading to *N*-arylation, annulative π-extension, or C–H fluorination.

Access to a high-level molecular complexity and diversity typically requires multi-step transformation processes involving functional group interconversion and protecting group chemistry.[1] In sharp contrast, direct (late-stage) diversification of a parent molecule can provide atom- and step-economic routes to afford various synthetic analogues.[2–5] To realize such strategies, a set of reliable and orthogonal reaction manifolds is essential. We envisioned that the combination of carefully selected transition-metal catalysts and intrinsic directing groups (DGs) would create opportunities to modulate intrinsic reactivities of a substrate, while alleviating the need for laborious synthetic manipulation steps.

Quinazolin-4(3*H*)-one is a privileged alkaloid scaffold in the context of the pharmacological potential for anticancer agents or kinase inhibitors.[6–9] Recently, palladium-catalyzed *O*-alkenylation and C–H arylation of quinazolinones have been reported.[10,11] The molecular structure possesses nucleophilic nitrogen, which can easily afford *N*-functionalized derivatives (Scheme 1, pathway (i)).[12] In addition, this substrate scaffold is endowed with intrinsic DGs that can promote tandem C–H arylation and C–H amidation (Scheme 1, pathway (ii)) or C–H fluorination (Scheme 1, pathway (iii)).[5,11,13,14] Herein, we report the development of straightforward diversification methods of unmasked 2-phenylquinazolin-4(3*H*)-ones via orthogonal reaction manifolds. This catalyst-controlled reactivity modulation strategy enables efficient and site-selective derivatizations of the alkaloid core scaffold without employing exogenous coordinating moieties or protecting groups.

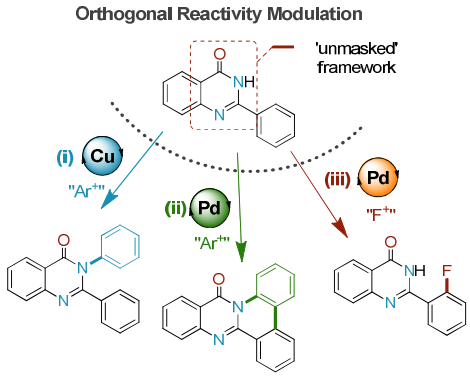

Scheme 1 Divergent pathways of a 2-phenylquinazolin-4(3*H*)-one.

Diversification of unmasked and readily available **1a** commenced with *N*-arylation using hypervalent diphenyliodonium triflate, which features bench stability and unique reactivity patterns.[15,16] We envisaged that the *N*-arylation could be achieved via the formation of a reactive aryl-copper(III) intermediate, as depicted in Table 1.[17–19] To our delight, the addition of 10 mol% copper iodide enabled direct access to the *N*-arylated product **2a** in 74% yield under aerobic conditions (Table 1, entry 1). As a control, metal-free conditions provided only a trace amount of **2a** (Table 1, entry 2). The addition of simple 2,2'-bipyridyl ligand **L1** slightly increased the yield (Table 1, entry 3), and ligand screening (Table 1, entries 4–9) revealed that quinoline-based **L7** performed the best, giving a yield of 93%.

Having optimized the *N*-arylation process, our attention shifted to the tandem synthesis of phenanthridine-fused derivative **3a** from **1a** (Table 2). There are two challenges associated with our direct oxidative annulation strategy,

[a] School of Energy and Chemical Engineering, Ulsan National Institute of Science and Technology (UNIST), 50 UNIST-gil, Ulsan 44919, Republic of Korea, E-mail: syhong@unist.ac.kr
[b] School of Materials Science and Engineering, UNIST, 50 UNIST-gil, Ulsan 44919, Republic of Korea, E-mail:jangung@unist.ac.kr
[c] Department of Chemistry, UNIST, 50 UNIST-gil, Ulsan 44919, Republic of Korea
[d] Center for Genomic Integrity (CGI), Institute for Basic Science (IBS), School of Life Science, UNIST, 50 UNIST-gil, Ulsan 44919, Republic of Korea

† Electronic Supplementary Information (ESI) available: Additional tables, experimental procedures, and NMR spectra. See DOI: 10.1039/x0xx00000x

View Article Online
DOI: 10.1039/C7CC05794F

namely (i) a sequential combination of C–H arylation and C–H amidation and (ii) competition with *ortho* di-arylation. Indeed, a few synthetic methods for this useful scaffold are reported, but only from prehalogenated substrates.[20,21] To our delight, the initial ligand-free screening conditions afforded the desired annulated product (Table 2, entry 1), albeit with a high catalyst loading. The formation of **3a** was restricted when bulky [MesIPh]OTf was employed (Table 2, entry 2). $Pd(OAc)_2$ was found to be the most effective catalyst (see the Supplementary Information, Table S1), and KOAc was the most suitable base for this reaction (Table 2, entry 3; Table S2). Other solvents and reaction temperatures were also screened, and DMF and 130 °C were selected (Table 2, entries 4, 5; Table S3). Increasing the amount of diphenyliodonium salt slightly decreased the yield of product **3a** (71%), owing to the formation of the di-arylated product **3a'** (8%) (Table 2, entry 6).

Table 1 Optimization of *N*-arylation[a]

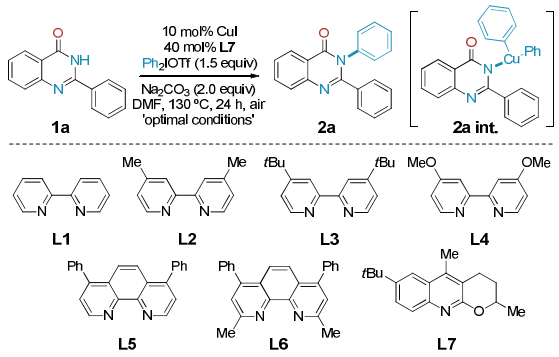

Entry	Catalyst	Ligand	Yield[b] (%)
1	CuI	–	74
2	–	–	3
3	CuI	**L1**	83
4	CuI	**L2**	65
5	CuI	**L3**	87
6	CuI	**L4**	75
7	CuI	**L5**	58
8	CuI	**L6**	67
9	**CuI**	**L7**	**93**

[a] Optimal conditions: **1a** (0.09 mmol, 1.0 equiv), Ph_2IOTf (0.135 mmol, 1.5 equiv), CuI (10 mol%), **L7** (40 mol%), Na_2CO_3 (0.18 mmol, 2.0 equiv), DMF (2.0 mL), 130 °C, 24 h, air. [b] Yield determined by GC analysis using *n*-dodecane as an internal standard. Tf, trifluoromethanesulfonyl.

When the catalyst loading was reduced to 10 mol%, the product was formed in a significantly diminished yield (37%) (Table 2, entry 7). We speculated that this low catalytic inefficiency is presumably linked to a Pd(II)/Pd(0) cycle of the C–H amidation (Scheme 2, cycle II) on the basis of previous literature reports,[22,23] where Pd(0) precipitation as Pd black may consume active catalysts. Yet, a Pd(II)/Pd(IV) manifold cannot be completely ruled out (see Section III.3 in the Supplementary Information, Scheme S1).[24] In order to test our hypothesis and address the catalyst loading issue, we decided to regenerate active Pd(II) species through terminal oxidation. After screening a series of oxidants, addition of 1.0 equivalent of silver trifluoroacetate (AgTFA) was found to be optimal, improving both the yield (74%) and the catalyst loading (Table 2, entry 8; Table S4). In addition, BrettPhos ligand led to the highest yield and reduced the amount of palladium catalyst (Table 2, entry 9; Table S5). Finally, our optimal conditions (Table 2, entry 10; Table S6) provided the desired annulated product in excellent yield (97%).

Table 2 Optimization of annulative π-extension[a]

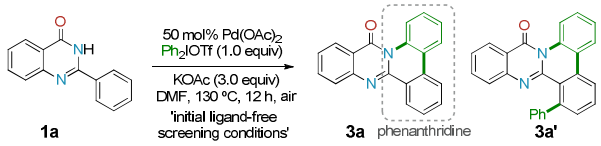

Entry	Deviation from the above initial ligand-free screening conditions	Yield[b] (%)
1	None	82
2	[MesIPh]OTf instead of Ph_2IOTf	–
3	NaOAc instead of KOAc	68
4	100 °C instead of 130 °C	27
5	DMSO instead of DMF	72
6	Ph_2IOTf (1.5 equiv)	71 (8)[c]
7	$Pd(OAc)_2$ (10 mol%)	37
8	$Pd(OAc)_2$ (20 mol%), AgTFA (1.0 equiv), 15 h	74
9	$Pd(OAc)_2$ (10 mol%), BrettPhos (40 mol%), Ph_2IOTf (1.2 equiv), AgTFA (1.0 equiv), 24 h	76[d]
10	**Optimal conditions: $Pd(OAc)_2$ (20 mol%), BrettPhos (30 mol%), Ph_2IOTf (1.1 equiv), AgTFA (1.0 equiv), KOAc (4.0 equiv), 24 h, O_2**	**97[d]**

[a] Optimal conditions: **1a** (0.09 mmol, 1.0 equiv), Ph_2IOTf (0.1 mmol, 1.1 equiv), $Pd(OAc)_2$ (20 mol%), BrettPhos (30 mol%), AgTFA (0.09 mmol, 1.0 equiv), KOAc (0.36 mmol, 4.0 equiv), DMF (2.0 mL), 130 °C, 24 h, O_2. [b] Yield determined by GC analysis using *n*-dodecane as an internal standard. [c] Di-arylated product **3a'**. [d] Isolated yield. Mes, 2,4,6-trimethylphenyl.

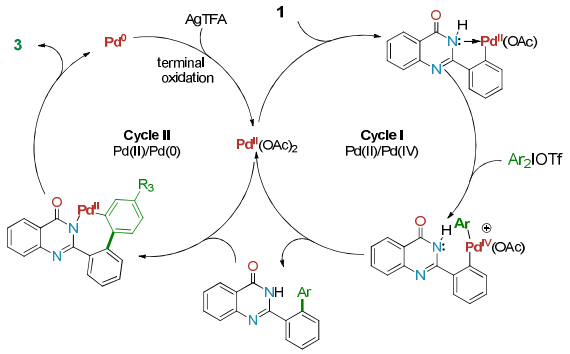

Scheme 2 Proposed mechanism of annulative π-extension.

With the optimal conditions in hand, the substrate scope of the annulation was examined (Scheme 3). The reactions proceeded smoothly under an oxygen atmosphere with a wide range of quinazolin-4(3*H*)-ones. Both electron-donating and

View Article Online
DOI: 10.1039/C7CC05794F

electron-withdrawing substituents such as methoxy (**3b**, **3c**), methyl (**3d**, **3e**), and nitro (**3f**) groups were well-tolerated (88–95%). Fluoro groups generally led to moderate to excellent yields (**3g**–**3j**). Remarkably, both chloro and bromo groups remained intact to give the corresponding products (**3k**–**3m**) in moderate to good yields (54–78%). These halides can be utilized as synthetic handles for further modifications. Di-substituted substrates (**3n**–**3p**) containing both electron-donating and electron-withdrawing groups showed similar or better reactivities.

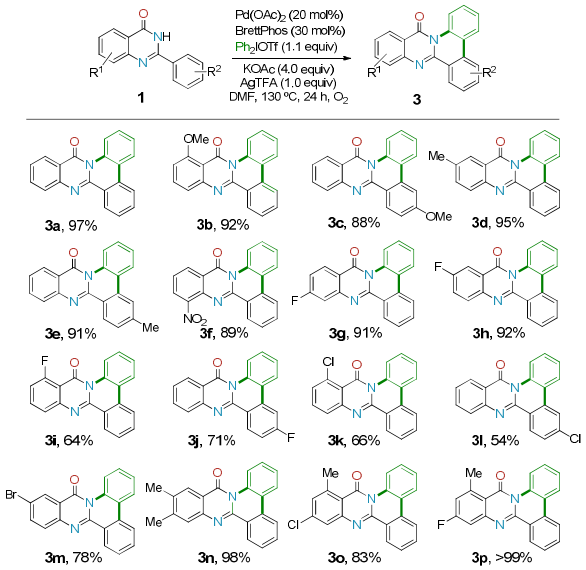

Scheme 3 Substrate scope of annulative π-extension and isolated yields of **3**.

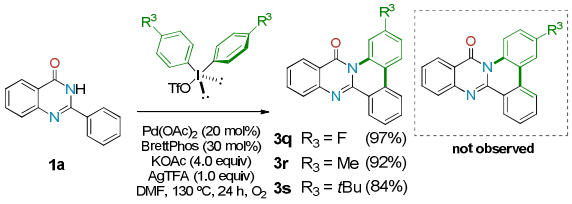

Scheme 4 Aryl transfer reactions with substituted iodonium salts.

The regioselectivity of aryl transfer reactions was also evaluated with substituted iodonium salts bearing fluoro, methyl, or *tert*-butyl groups (Scheme 4). Notably, these iodonium salts invariably afforded the corresponding products as a single isolated regioisomer (**3q**–**3s**). The exclusive regioselectivity clearly indicates the tandem sequence of intermolecular C–C bond formation, and subsequent intramolecular C–N bond formation (see also the aforementioned Scheme 2).

As the next diversification pathway, we set out to investigate C–H fluorination. Efficient incorporation of fluorine functionalities into bioactive molecular scaffolds has undisputable significance in pharmaceuticals, since it confers the lipophilicity and metabolic stability.[25] The Yu and Sanford groups independently developed C–H fluorination methods involving high-valent transition-metal catalysis.[26–28] After screening of reaction conditions, fluorinated **4a** was obtained in 91% yield under aerobic conditions (Table 3, entry 1). Control experiments involving the alteration of the electrophilic fluorinating reagent, temperature, and solvent invariably led to reduced yields (Table 3, entries 2–8).

Table 3 Optimization of C–H fluorination[a]

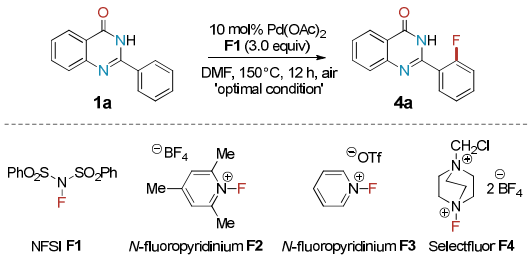

Entry	Deviation from the above optimal conditions	Yield[b] (%)
1	**None**	**91**
2	**F2** instead of **F1**	13
3	**F3** instead of **F1**	1
4	**F4** instead of **F1**	–
5	1.5 equiv of **F1** instead of 3.0 equiv	63
6	MeCN instead of DMF	39
7	100 °C instead of 150 °C	58
8	24 h at 130 °C instead of 12 h at 150 °C	38

[a] Optimal conditions: **1a** (0.09 mmol, 1.0 equiv), NFSI **F1** (0.27 mmol, 3.0 equiv), $Pd(OAc)_2$ (10 mol%), DMF (2.0 mL), 150 °C, 12 h, air. [b] Yield determined by GC analysis using *n*-dodecane as an internal standard. NFSI, *N*-fluorobenzenesulfonimide.

To highlight the synthetic utility, we applied our annulation product to a chemically-modified graphene-FET device for the nanoelectronic detection of metal ions as illustrated in Fig. 1a. A phenanthridine-fused **3a** was noncovalently incorporated into the graphene-FET through the π-π interaction. A microfluidic channel was integrated onto the chemically-modified graphene-FET (Fig. 1b). As shown in Fig. 1c, the addition of a Hg^{2+} solution (100 ppm) into the microfluidic channel changed the current (ΔI_D). A positive shift of ~0.2 V in the Dirac voltage was observed upon binding of Hg^{2+}. In contrast, the **3a**-modified graphene-FET sensor showed a negative shift in the Dirac voltage for Na^+, K^+, and Cu^{2+} ions (Fig. S1). The phenomenon is presumably associated with the metal-dependent coordination of heterocyclic **3a**, affecting the current in the conductive channel.[29,30] To investigate the reversibility of the sensors further, imidazole aqueous solution was consecutively injected to wash out the immobilized Hg^{2+}.[31] As a result, the current level of the device was recovered to the original state (Fig. 1d).

View Article Online
DOI: 10.1039/C7CC05794F

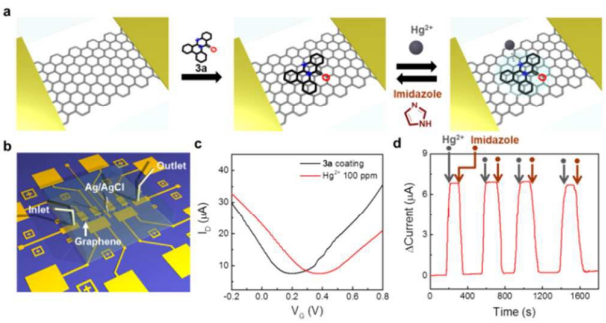

Fig. 1 (a) Schematic illustration. (b) Graphene-FET sensor. (c) Transfer (I_D-V_G) characteristics (V_D = 0.1 V). (d) Highly reversible Hg^{2+} sensing.

In conclusion, we have demonstrated the facile diversification of unmasked 2-phenylquinazolin-4(3*H*)-ones, a privileged alkaloid scaffold endowed with intrinsic coordinating moieties. Transition-metal catalyst-controlled reactivity modulation enabled access to the derivatives of the molecular framework via *N*-arylation, annulative π-extension, and C–H fluorination in a straightforward manner. The reactions were performed with no special equipment to exclude air or moisture. Finally, the synthetic value of a phenanthridine-fused quinazolinone derivative was featured by the construction of a chemically-modified graphene-based nanoelectronic device, which allowed real-time electronic recognition of Hg^{2+} ions in aqueous solution.

This work was supported by the National Research Foundation of Korea (NRF-2016R1A2B4015497) and the IT R&D program of MOTIE/KEIT (10046306). We are grateful to Prof. R. Tenne for his helpful comments.

Notes and references

1 S. L. Schreiber, *Science*, 2000, **287**, 1964.
2 H. Kondo, K. Itami and J. Yamaguchi, *Chem. Sci.*, 2017, **8**, 3799.
3 S. Mai and Q. Song, *Angew. Chem., Int. Ed.*, 2017, **56**, 7952.
4 X.-H. Liu, H. Park, J.-H. Hu, Y. Hu, Q. L. Zhang, B. L. Wang, B. Sun, K.-S. Yeung, F.-L. Zhang and J.-Q. Yu, *J. Am. Chem. Soc.*, 2017, **139**, 888.
5 T. Truong and O. Daugulis, *Chem. Sci.*, 2013, **4**, 531.
6 K. Upadhyaya, R. K. Thakur, S. K. Shukla and R. P. Tripathi, *J. Org. Chem.*, 2016, **81**, 5046.
7 H. Wang, X. Cao, F. Xiao, S. Liu and G.-J. Deng, *Org. Lett.*, 2013, **15**, 4900.
8 X. Liu, H. Fu, Y. Jiang and Y. Zhao, *Angew. Chem., Int. Ed.*, 2009, **48**, 348.
9 T. Abe, K. Kida and K. Yamada, *Chem. Commun.*, 2017, **53**, 4362.
10 R. Lingayya, M. Vellakkaran, K. Nagaiah, P. R. Tadikamalla and J. B. Nanubolu, *Chem. Commun.*, 2017, **53**, 1672.
11 D. N. Garad, A. B. Viveki and S. B. Mhaske, *J. Org. Chem.*, 2017, **82**, 6366.
12 H. C. Ma and X. Z. Jiang, *Synlett*, 2008, 1335.
13 H. M.-F. Viart, A. Bachmann, W. Kayitare and R. Sarpong, *J. Am. Chem. Soc.*, 2017, **139**, 1325.
14 F. Zhang and D. R. Spring, *Chem. Soc. Rev.*, 2014, **43**, 6906.
15 E. A. Merritt and B. Olofsson, *Angew. Chem., Int. Ed.*, 2009, **48**, 9052-9070.
16 N. R. Deprez and M. S. Sanford, *Inorg. Chem.*, 2007, **46**, 1924.
17 S. R. Chemler, *Science,* 2013, **341**, 624.
18 L. M. Huffman and S. S. Stahl, *J. Am. Chem. Soc.,* 2008, **130**, 9196.
19 S.-K. Kang, S.-H. Lee and D. Lee, *Synlett,* 2000, **2000**, 1022.
20 B. Banerji, S. Bera, S. Chatterjee, S. K. Killi and S. Adhikary, *Chem. Eur. J.,* 2016, **22**, 3506.
21 P. K. Gupta, N. Yadav, S. Jaiswal, M. Asad, R. Kant and K. Hajela, *Chem. Eur. J.,* 2015, **21**, 13210.
22 J. Karthikeyan and C.-H. Cheng, *Angew. Chem., Int. Ed.,* 2011, **50**, 9880.
23 G.-W. Wang, T.-T. Yuan and D.-D. Li, *Angew. Chem., Int. Ed.,* 2011, **50**, 1380.
24 M. Wasa and J.-Q. Yu, *J. Am. Chem. Soc.,* 2008, **130**, 14058.
25 M. G. Campbell and T. Ritter, *Chem. Rev.,* 2015, **115**, 612.
26 A. J. Hickman and M. S. Sanford, *Nature,* 2012, **484**, 177.
27 X. Wang, T.-S. Mei and J.-Q. Yu, *J. Am. Chem. Soc.,* 2009, **131**, 7520.
28 K. L. Hull, W. Q. Anani and M. S. Sanford, *J. Am. Chem. Soc.,* 2006, **128**, 7134.
29 H. G. Sudibya, Q. He, H. Zhang and P. Chen, *ACS Nano* 2011, **5**, 1990.
30 O. Knopfmacher, M. L. Hammock, A. L. Appleton, G. Schwartz, J. Mei, T. Lei, J. Pei and Z. Bao, *Nat. Commun.,* 2014, **5**, 2954.
31 A. S. Knight, R. U. Kulkarni, E. Y. Zhou, J. M. Franke, E. W. Miller and M. B. Francis, *Chem. Commun.,* 2017, **53**, 3477.